

Filling and Emptying of Gravure Cells – Experiment and CFD Comparison*

J. M. Brethour[†] and H. Benkreira[‡]

[†]Flow Science, Inc., 683A Harkle Road, Santa Fe, New Mexico USA 87505

[‡]Department of Chemical Engineering, University of Bradford, West Yorkshire UK BD7 1DP

Abstract

This work brings to bear the power of modern computational fluid dynamics onto complex coating flows. In this paper, a fully three-dimensional transient model based on the Navier-Stokes system of equations is presented along with a simple, yet powerful, treatment of dynamic contact lines. Also included is a model to predict the effect of air trapped behind the wetting line.

In gravure coating, the gravure cells do not completely fill with coating liquid beneath the doctor blade nor does all of the fluid leave the cell onto the substrate or applicator. Few studies have dealt with individual cell filling and withdrawal. Much research on gravure coating involves experimental measurements to determine the fractional volume of the cells applied to the substrate or transfer roll; this varies for different cell shapes and sizes, and roll speed. L. W. Schwartz et al [1] presented mathematical models of cell drainage and withdrawal with simplified flow models; however, their work does not consider the effects of entrapped air or inertia on the flow.

Introduction

Treatment of dynamic wetting lines

At dynamic wetting lines, there should be no velocity slip at the microscopic scale. However, continuum flow models that impose the no-slip condition at the wetting line result in a singularity there [2,3]. It should be pointed out that this singularity is confined to a molecular scale region near the dynamic wetting line where the continuum model is not valid. In this work a finite-control-volume technique is used. This method does not impose specific flow values at any point but rather keeps track of the mass and momentum in each control volume element. The location of fluid interfaces is tracked by a volume-of-fluid (VOF) method in which the *fluid fraction* within each control volume is computed and stored. Based on the fluid fractions of neighboring cells, free surfaces are located, and surface slopes and curvatures can be computed [4]. At contact lines, an additional force describing the adhesion between the solid and the liquid is added to the dynamic processes of mass and momentum conservation. Adhesion forces are assumed to arise from molecular interactions between the solid and liquid. This interaction is characterized by the static contact angle because the molecular processes that cause the adhesion force act at a space and time scale far smaller and faster than those of the continuum flow process. Therefore, the wall adhesion force is computed from the cosine of the static contact angle and the interfacial tension between the air and the liquid [5]. The resulting sum of forces at the dynamic wetting line produces a prediction of the dynamic contact angle based on only one parameter, the static contact angle.

To further understand how this dynamic wetting model works, Figure 1 shows results for the tape plunging problem — mylar (polyethylene terephthalate) film is drawn into a pool of an aqueous glycerol solution. The capillary number is based on the speed of the film. Data from both the numerical model and experiment are shown. Measurements [6] show a gradual rise in the dynamic contact angle from the equilibrium static angle even at capillary number values below 0.001. This is followed by a steeper rise in the contact angle beginning at a capillary number of about 0.01. Figure 2 shows a comparison for a different experiment — liquid driven through a capillary. Measurements [6] here again show a gradual rise in contact angle at Ca less than 0.05, beyond which the contact angle rises more steeply until it approaches 180° . The model does predict the trend in contact angle well for high capillary numbers, but does not predict the gradual rise in contact angle at low capillary numbers.

In the hydrodynamic theory [6], the dynamic contact angle only begins to rise when viscous forces become large enough to compete with surface tension forces. Since the capillary number is a measure of the relative importance of these two forces, it is hard to explain the change in measured contact angle at capillary number below 0.01 unless something alters the liquid-solid adhesion force. Simple molecular interactions between liquid and solid occur at time and space scales orders of magnitude faster and

* Presented at the 11th International Coating Science and Technology Symposium, September 23-25, 2002, Minneapolis, Minnesota. Unpublished. ISCST shall not be responsible for statements or opinions contained in papers or printed in its publications.

smaller than even microscopic observations of the contact angle. The effect of microscopic surface roughness may be significant. The presence of roughness causes the advancing contact line to pin to the roughness elements giving the appearance of a larger effective contact angle [7,8]. These roughness elements can also explain the difference in observed dynamic contact angles between dry and pre-wetted surfaces: the microscopic pits contain air on dry surfaces so the liquid tends to bridge these gaps resulting in a larger contact angle [7], while pre-wetted surfaces contain liquid in the pits allowing the liquid to adhere to the entire surface, lowering the apparent contact angle.

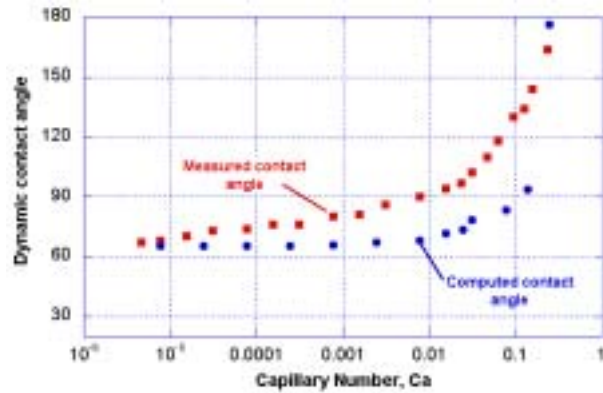


Figure 1. Comparison of mylar tape plunging experimental measurements [6] to model results for various contact angles. The static contact angle is 64.5° and the capillary number is based on the tape speed.

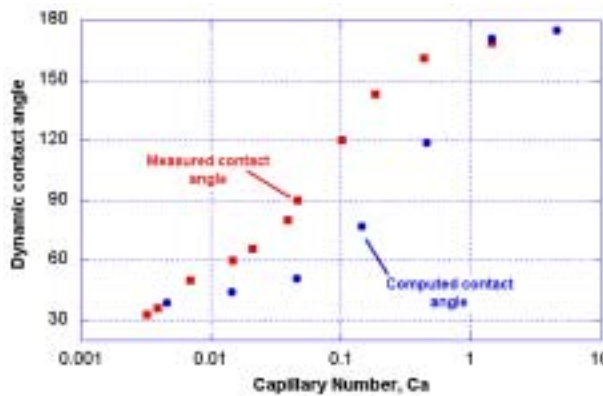


Figure 2. Dynamic contact angle from experimental measurements [6] and model for liquid driven through a capillary. The static contact angle is 0° and the capillary number is based on the mean flow velocity.

The flow model as presented here is able to predict dynamic contact angles for varying capillary numbers that exhibit the same qualitative behavior as experimental measurements. However, the quantitative predictions at low capillary numbers under predict the dynamic contact angle possibly because of microscopic surface roughness effects.

Gravure coating

Gravure roll coating is commonly used where low coat weights are to be applied at high speed. In such situations, roll coating can be problematic because the coat weight is sensitive to the intricate balance of viscous, capillary and inertial forces within the roll gap. Slight changes in speed or roll gap can drastically affect the final coating thickness when the desired coating thickness is small. With gravure rolls, most of the coating fluid is contained within the gravure cells, which is a fixed volume for each roll. Therefore, the final coat weight is less a function of poorly controlled parameters (fluid viscosity, surface tension and roll speed) and more a function of the cell geometry, which can be finely controlled for each application.

In gravure roll coating, the key to understanding how the cells fill and empty is to study the processes occurring within individual cells. This is very difficult to do experimentally because of the minute size of

the gravure cells: they are typically less than 200 μm across. Also, the speed at which a gravure roll rotates makes visualization of the fluid motion in individual cells virtually impossible. Therefore, little study has been done of the cell filling and emptying of individual gravure cells. Schwartz [1] presented a numerical model of the gravure cell withdrawal process; this work did not include effects of entrapped air within the cell or the effects of inertia.

In the gravure coating process, air can become trapped. In this model, the trapped air behaves isentropically with $PV^{1.4}$ held constant to control the pressure-volume relation within bubbles. There is no transfer of energy or mass between the fluid and the gas bubble. In open gas regions, the gas pressure is fixed to be atmospheric.

All of the simulations presented here were computed using the control-volume-VOF method as it has been implemented in the commercial software package **FLOW-3D**[®] developed by Flow Science, Inc., Santa Fe, New Mexico, USA [9].

Filling of a Gravure Cell

Within the grid of finite control volume elements, one gravure cell was created by blocking off flow to elements located within solid regions, and those elements partly blocked by the solid are partially blocked to flow by manipulating the area fractions open to flow in each of the three Cartesian directions. Quadrangular gravure cells were used for the simulations. The spacing between each cell is $130\mu\text{m}$ and the depth of each cell is $32\mu\text{m}$. The cell volume per unit area of roller surface (V_c) is $13.25 \times 10^{-6} \text{m}^3/\text{m}^2$ and the fraction of roller area that is gravure cells is 0.809. Also created within the mesh is a rigid solid blade, which translates downward in the model. The minimum gap between the blade and the gravure roll surface is $2\mu\text{m}$. The fluid's viscosity is $10\text{mPa}\cdot\text{s}$, its density is $1\text{g}/\text{cm}^3$ and the air-liquid surface tension is $40\text{mN}/\text{m}$. The static contact angle between the liquid and the blade is 30° for all cases. The static contact angle between the liquid and the gravure roll and the roll speed varies.

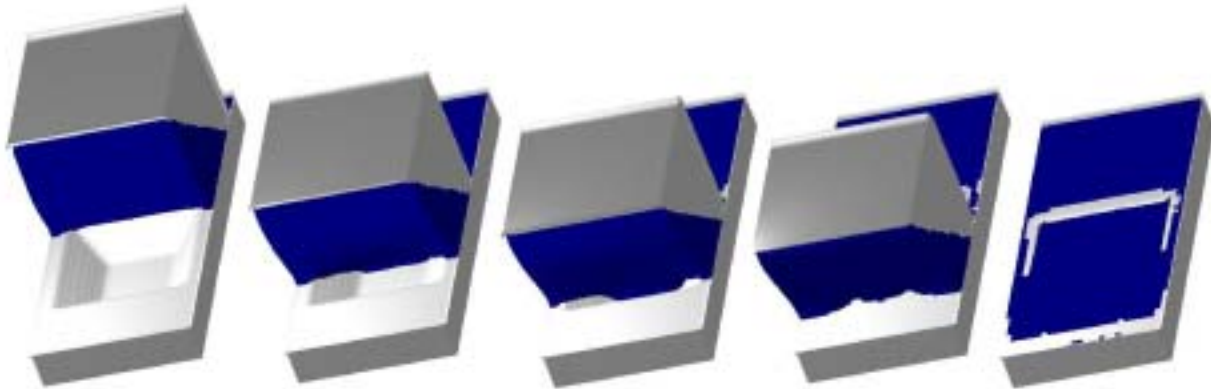


Figure 3. Three-dimensional view of a quadrangular gravure cell filling at $1\text{m}/\text{s}$. The elapsed time here is $400\mu\text{s}$.

Figure 3 shows the time evolution of the cell filling process; the static contact angle with the gravure roll is 30° , the roller speed is $1\text{m}/\text{s}$ and the gap between the blade and the gravure roller is $2\mu\text{m}$. In this case, the advancing contact line at the front edge of the liquid bead is able to move into the gravure cell quickly enough so that air is not trapped by the leading edge of liquid entering the cell. After the blade has passed over the cell, the liquid overlying the cell edges thins due to the capillary pressure driving fluid away under the curved surface. Greatest fill fractions are obtained at low roll speeds and low static contact angles. Low roll speeds allow the advancing contact to enter farther into the cell before the air is trapped by the liquid bead being pushed by the blade. Low contact angles result in faster advancement of the contact line.

Emptying of a Gravure Cell

Again, a gravure cell of the same dimensions was created within the grid of finite control volumes, but instead of a translating blade, the pulling away of the substrate from the surface of the gravure roll was

modeled by creating a solid block that translates linearly away from the roll. This motion is adequate to describe the separation because at such small scales the transfer roll would appear to move linearly away from the gravure roll. Also, the fluid initially in the cell was presumed from the results of the gravure filling simulations. Figure 4 shows the case where the transfer roll is pulling away at 0.5m/s and the static contact angle with all surfaces is 30°.

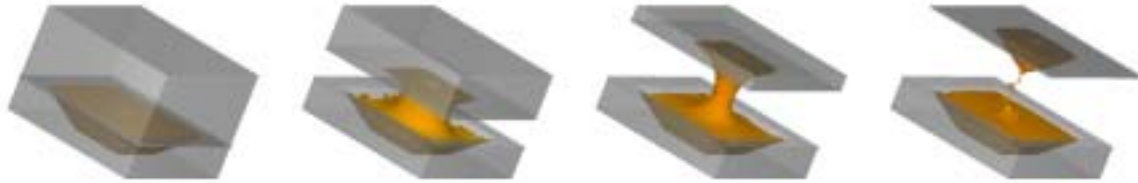


Figure 4. Emptying of gravure cell (same cell dimensions as filling case); a three-dimensional perspective is shown. The transfer roll surface (block at top) is moving away from the gravure roll at 0.5m/s. The static contact of the fluid with all surfaces is 30°. The elapsed time is 150 μ s.

These results show the necking of the liquid as it pulls away from the gravure cells. A fraction of the liquid adheres to the transfer roll. Also, higher speeds and/or higher contact angles to the transfer roll surface cause the volume of fluid adhering to the transfer roll to fall. Results comparing this applied fraction to experimental measurement of film thickness will be presented.

Summary

A numerical simulation method of the filling and emptying of individual gravure cells has been performed for a variety of sample cases showing the effect of the static contact angle (with the gravure roll surface) and the speed of roll rotation. The advantage of this method is the ability to study the movement of free surfaces into the cell on any time scale with any cell geometry with any desired fluid. This is not possible with existing fluid visualization techniques.

The results demonstrate how roll speed and the static contact angle affect the movement of fluid into the gravure cell. Lower static contact angles and low speeds are most conducive to ensuring maximum fill or emptying of the cells because the advancing contact line is able to move into the cell before the liquid bead traps air inside. Because the model approach described in this paper exists in a commercial software package [9], it is available for immediate application to the investigation of quality issues associated with many types of coating applications.

References

1. Schwartz, L.W., Moussalli, P., Campbell, P. and Eley, R. R., Numerical modelling of liquid withdrawal from gravure cavities in coating operations, *Trans IChemE*, **76(A)**, 22-28 (1998)
2. Huh, C. & Scriven, L. E. Hydrodynamic model of steady movement of a solid/liquid/fluid contact line, *J. Colloid Interface Sci.* **35**, 85 (1971).
3. Dussan V., E. and Davis, S. H. On the motion of a fluid-fluid interface along a solid surface, *J. Fluid Mech.* **65**, 71 (1974).
4. Hirt, C.W. and Chen, K.S., Simulation of slide-coating flows using a fixed grid and a volume of fluid front-tracking technique, *Proc. 8th International Symposium on Coating Science and Technology*, New Orleans (1996)
5. Young, T., An essay on the cohesion of fluids, *Phil. Trans. Royal Soc. (London)*, **95**, p. 65 (1805)
6. Blake, T. D. and Ruschak, K. J. Wetting: Static and Dynamic Contact Lines, *Liquid Film Coating*, Kistler, S. F. and Schweizer, P. M. eds. Chapman & Hall, London (1997)
7. Hirt, C. W. and Brethour, J. M. Contact lines on rough surfaces and application to air entrainment, *Proc. 11th International Symposium on Coating Science and Technology*, Minneapolis (2002).
8. Hocking, L. M. A moving fluid interface on a rough surface. *J. Fluid Mech.*, **76**, 801 (1976).
9. **FLOW-3D**[®] User's Manual, *Flow Science, Inc. report FSI-02-1* (2002), www.flow3d.com.